Supporting Information

Two-dimensional semiconducting Cu(I)-MOF for binder and conductive additive-free supercapattery

Shivendu Mishra[a], Mayank K. Singh[b], Dilip Pandey[a], Dhirendra K. Rai*[b], Abhinav Raghuvanshi*[a]

[a]*Department of Chemistry, Indian Institute of Technology Indore, Simrol, Indore, Madhya Pradesh, 453552, India.*

[b]*Sustainable Energy and Environmental Materials (SEEM) Lab, Department of Metallurgical Engineering and Material Science, Indian Institute of Technology Indore, Simrol, Indore, Madhya Pradesh, 453552, India.*

Email- dkrai@iiti.ac.in (DKR); r.abhinav@iiti.ac.in (AR)

Table of contents

General Information

Materials

We used two neck round bottom flask, dried at 80 °C for 12 hours, for ligand synthesis and a Schlenk tube for the synthesis of MOF. The reactions have been performed using Schlenk line technique under N_2 atmosphere. Materials required for the synthesis of ligands such as 2-bromopyridine (>99%) were purchased from Spectrochem Pvt. Ltd. (India) and used without further purification. Cesium carbonate (>99%), CuI (>99%) were purchased from Loba Chemie Pvt. Ltd., Dimethyl formamide (DMF) were bought from Advent Chembio Pvt. Ltd., acetonitrile HPLC grade from Finar Chemicals Pvt. Ltd. and deuterated solvents $CDCl_3$ with 0.03 % TMS as an internal standard were purchased from Eurisotop and used without further purification.

Characterization methods

The characterization of ligand is done on a Bruker Avance Neo NMR spectrometer operating at 400 MHz and Bruker-Daltonic-Micro-TOF-QII mass spectrometer for exact mass and isotopic measurement. Dual source Super Nova CCD (Agilent Technologies (Oxford Diffraction) is used for Single crystal X-Ray data using Mo-Kα= 0.71073 at 293 K. The structure solution was obtained by using OLEX software and the SHELXT structure solution program using Intrinsic Phasing and refined with the SHELXL refinement package using Least Squares.[1-2]

Synthesis of 2-(1H-1,2,4-triazol-1-yl)pyridine (2TzPy)

We have synthesized the molecularly rigid multidentate ligand 2-(1H-1,2,4-triazol-1-yl)pyridine (2TzPy) by following a procedure reported in the literature.[3] In a two-neck round bottom flask, dried overnight at 80 °C prior to the reaction, added 1H-1,2,4-triazole (4.8 mmol, 331.5 mg), Cs_2CO_3 (6.138 mmol, 2g), CuI (0.76 mmol, 145 mg) and 2-bromopyridine (4 mmol, 395 µL). The reaction mixture was heated in 15 mL DMF at 140 °C for 40 h, and the reaction was monitored by TLC. Before the final work-up process, the DMF was removed through vacuum distillation connected through a Schlenk line. The reaction mixture was diluted in ethyl acetate, passed through a celite pad, and extracted with a brine solution and water. The final product is passed through silica in ethyl acetate: hexane (40:60) to get the desired product in 87 % yield. The product formation was confirmed by ^{1}H NMR and mass spectrogram, which matches with the reported literature.

Table S1. Crystallographic parameters of **CuCN-MOF**

CCDC No.	**2245742**
Empirical formula	$C_9H_6Cu_2N_6$
Formula weight	325.28
Temperature/K	293(2)
Crystal system	Triclinic
Space group	$P\bar{1}$
a/Å	8.2045(18)
b/Å	8.2891(9)
c/Å	9.0520(14)
α (°)	68.939(12)
β (°)	85.740(16)
γ (°)	72.413(15)
V (Å^3)	547.23(17)
Z	2
ρ_{calc} (g/cm^3)	1.974
F(000)	320.0
Radiation	Mo Kα (λ = 0.71073)
$2\theta_{max}$ (°)	5.902 to 54.996
Index ranges	$-10 \leq h \leq 10$, $-10 \leq k \leq 10$, $-11 \leq l \leq 11$
R1, wR2 [I>2σ(I)]	0.0654, 0.1415
R1, wR2 [all data]	0.1014, 0.1627
Reflections collected	4779
Independent reflections	2430 [R_{int} = 0.0668, R_{sigma} = 0.1044
Goodness-of-fit on F^2	0.990
Largest diff. peak/hole e Å^{-3}	0.90/-1.10

Table S2. Important bond-lengths.

Cu1-Cu1^1	2.4476(17)	N2-C7	1.341(8)
Cu1-N4	2.070(5)	N3-Cu2^4	2.153(4)
Cu1-N5	1.930(5)	N3-C6	1.322(7)
Cu1-C8^1	2.281(8)	N4-C6	1.357(8)
Cu1-C8	1.979(6)	N4-C7	1.318(7)
Cu2-N1^2	2.134(5)	N5-C9	1.161(8)
Cu2-N3^2	2.153(5)	N6-Cu2^5	2.004(6)
Cu2-N6^3	2.004(6)	N6-C8	1.153(9)
Cu2-C9	1.874(6)	C1-C2	1.380(9)
N1-Cu2^4	2.134(5)	C2-C3	1.386(9)
N1-C1	1.324(8)	C3-C4	1.383(10)
N1-C5	1.339(8)	C4-C5	1.359(9)
N2-N3	1.370(7)	C8-Cu1^1	2.281(8)
N2-C1	1.431(7)		

Symmetry operation code- ^{1}- *x*, 1 - *y*, - *z*; ^{2} + *x*, 1 + *y*, - 1 + *z*; ^{3} + *x*, 1 + *y*, + *z*; ^{4} + *x*, - 1 + *y*, 1 + *z*; ^{5} + *x*, - 1 + *y*, + *z*

Table S3. Selected bond angles.

N4-Cu1-Cu1[1]	110.86(15)	N2-N3-Cu2[4]	11.7(4)
N4-Cu1C8[1]	94.2(2)	C6-N3-Cu2[4]	144.2(5)
N5-Cu1-Cu1[1]	135.71(18)	C6-N3-N2	102.9(5)
N5-Cu1-N4	109.7(2)	C6-C4-Cu1	123.6(4)
N5-Cu1-C8[1]	110.9(2)	C7-C4-Cu1	132.9(4)
N5-Cu1-C8	118.3(3)	C6-C4-C6	102.9(5)
C8[1]-Cu1-Cu1[1]	49.33(16)	C9-N5-Cu1	177.4(6)
C8-Cu1-Cu1[1]	61.0(2)	C8-N6-Cu2[5]	166.9(5)
C8[1]-Cu1-N4	110.9(2)	N1-C2-N2	115.3(5)
C8-Cu1-C8[1]	110.3(2)	N1-C1-C2	124.2(6)
N1[2]-Cu2-N3[2]	76.6(2)	Cu1-C8-Cu1[1]	69.7(2)
N6[3]-Cu2-N1[2]	100.6(2)	N6-C8-Cu1	151.4(7)
N6[3]-Cu2-N3[2]	106.5(2)	N6-C8-Cu1[1]	138.9(6)
C9-Cu2- N1[2]	128.9(2)	N5-C9-Cu2	174.5(6)
C9-Cu2- N3[2]	121.4(2)		
C9-Cu2- N6[3]	115.5(3)		
C1-N1-Cu2[4]	116.1(4)		
C5-N1-Cu2[4]	126.5(4)		

Symmetry operation code- [1] - *x*, 1 - *y*, - *z*; [2] + *x*, 1 + *y*, - 1 + *z*; [3] + *x*, 1 + *y*, + *z*; [4] + *x*, - 1 + *y*, 1 + *z*; [5] + *x*, - 1 + *y*, + *z*

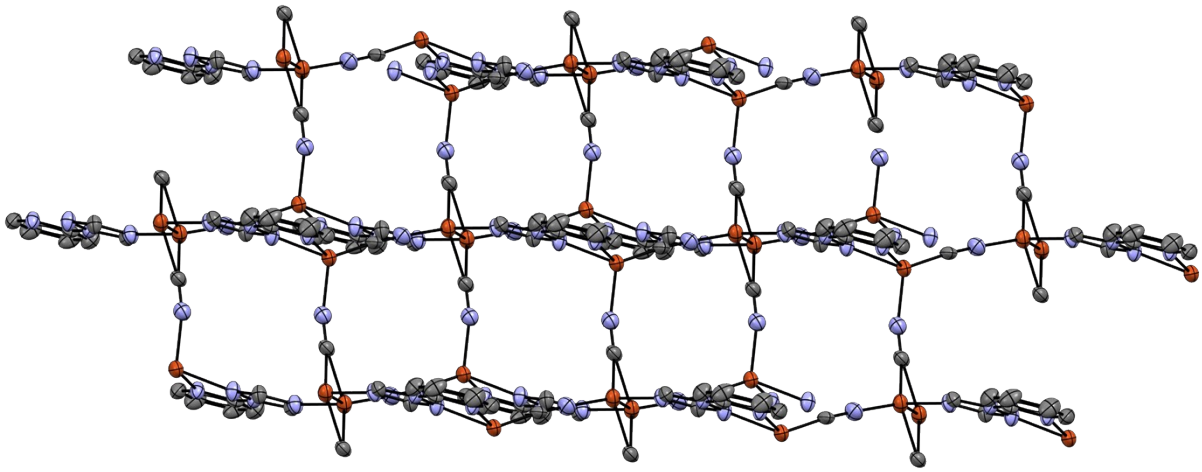

Figure S1. Crystal structure arrangement of **CuCN-MOF** showing different layers bridged by CN^- ion.

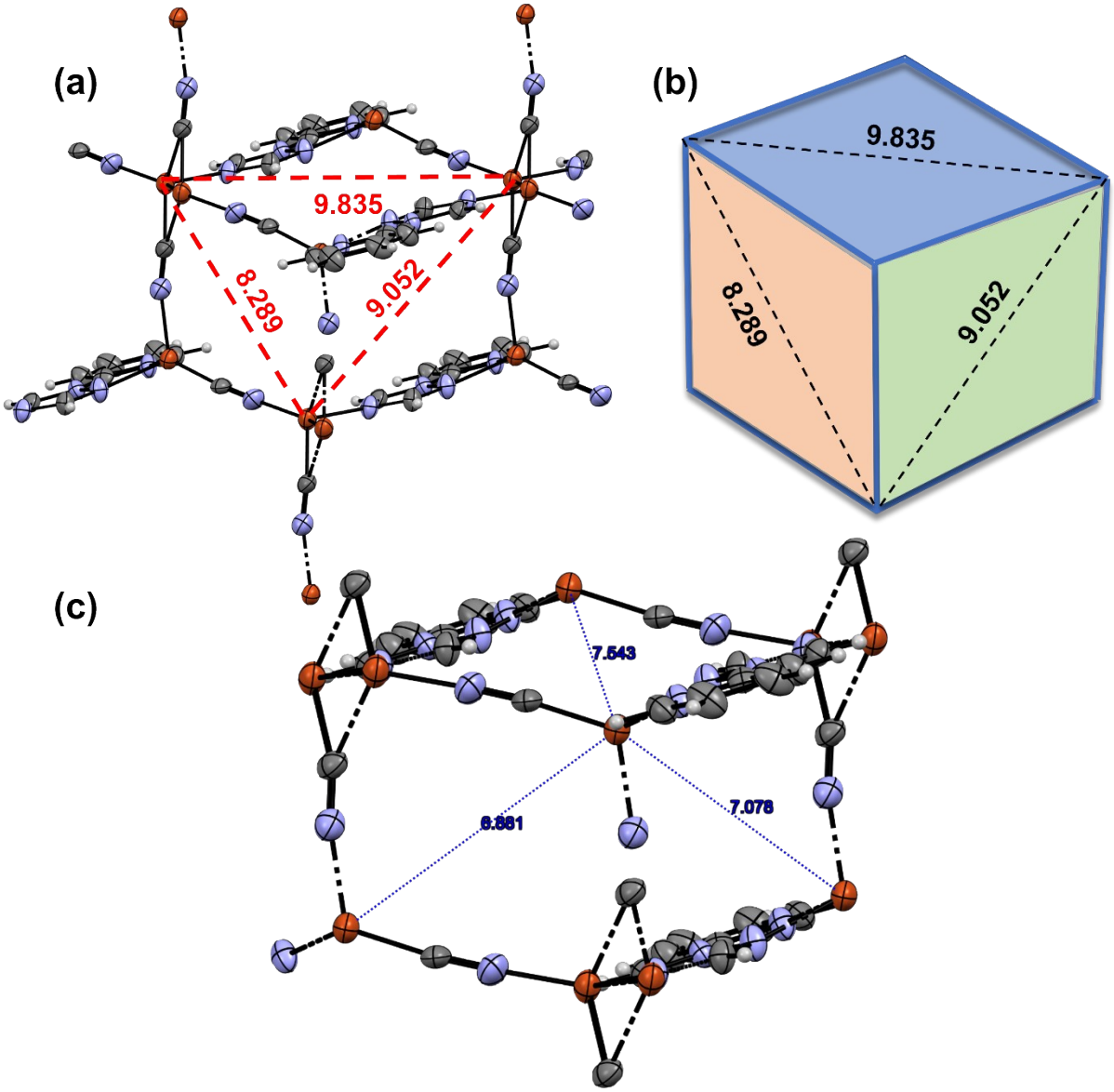

Figure S2. Cu-Cu distances in all three rectangular faces.

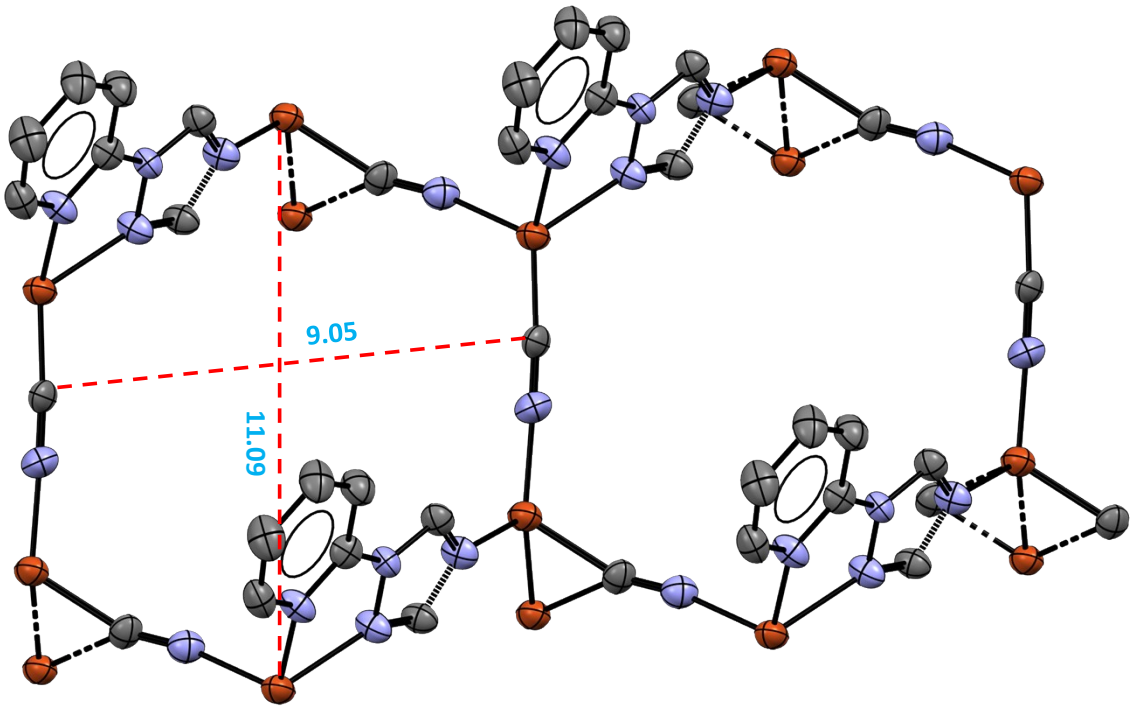

Figure S3. Open void present in one unit of the **CuCN-MOF**.

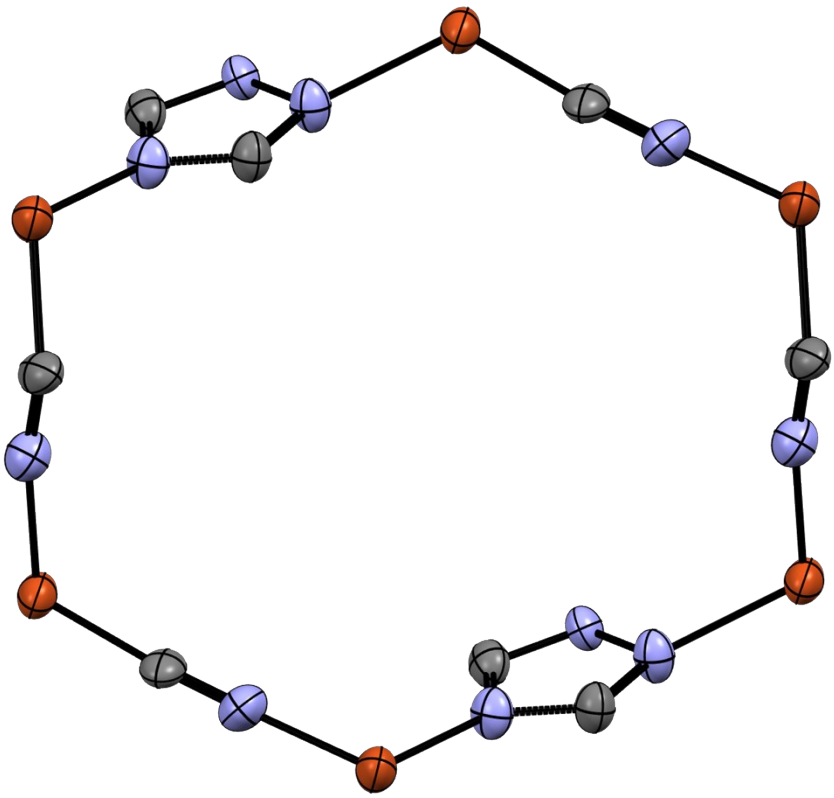

Figure S4. Largest metallacycle present in the **CuCN-MOF**.

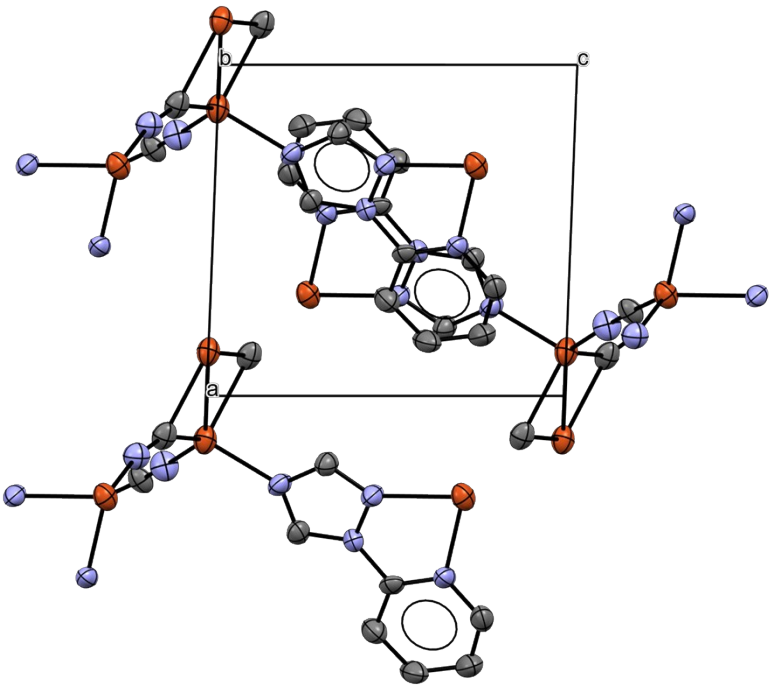

Figure S5. Crystal packing along b-axis.

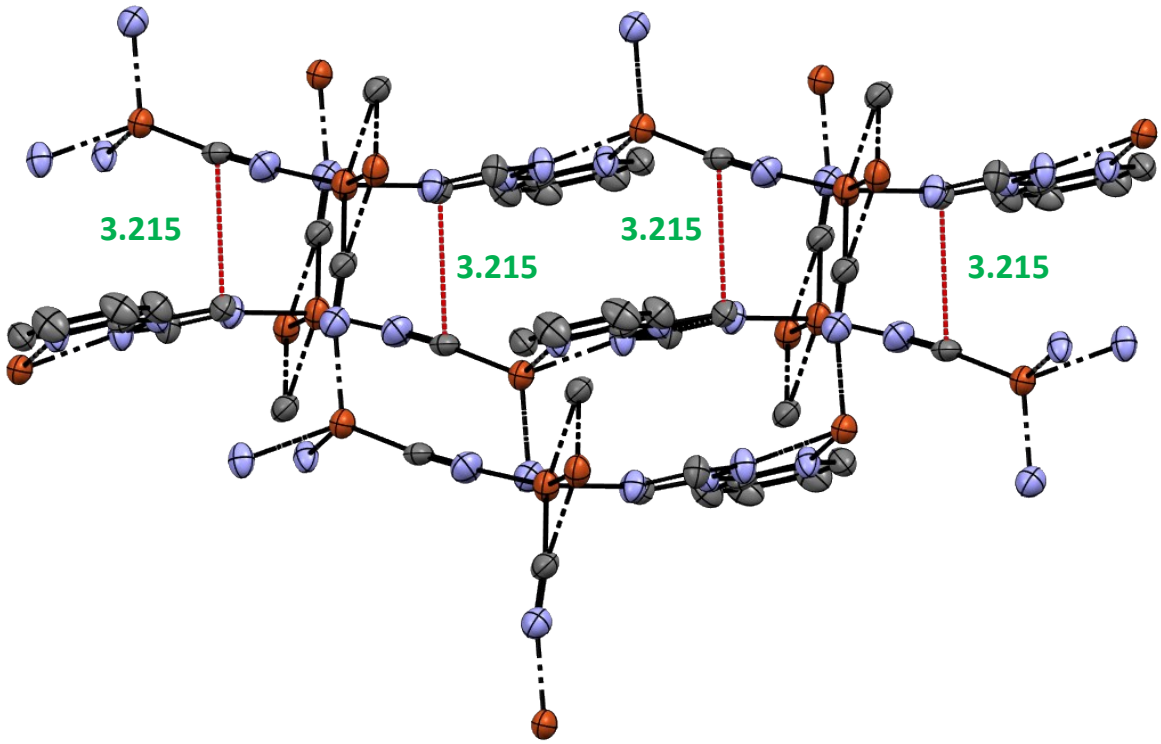

Figure S6. π-π stacking present in two different layers.

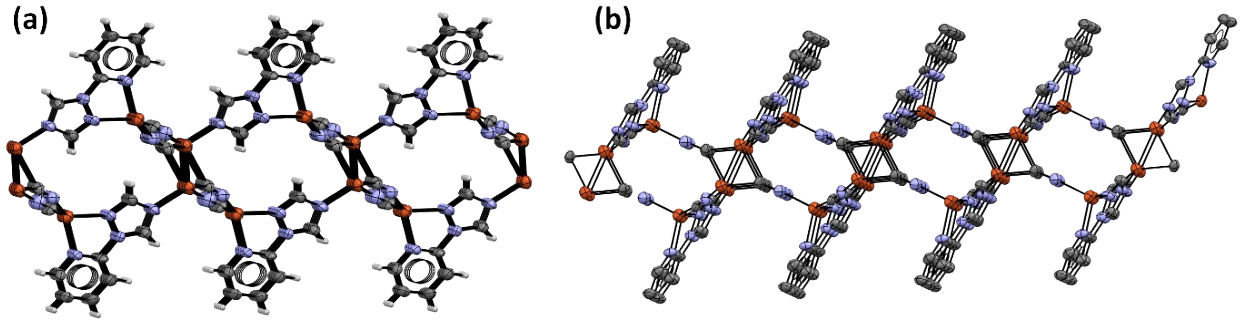

Figure S7. Pictures confirming 2D structure along different axes.

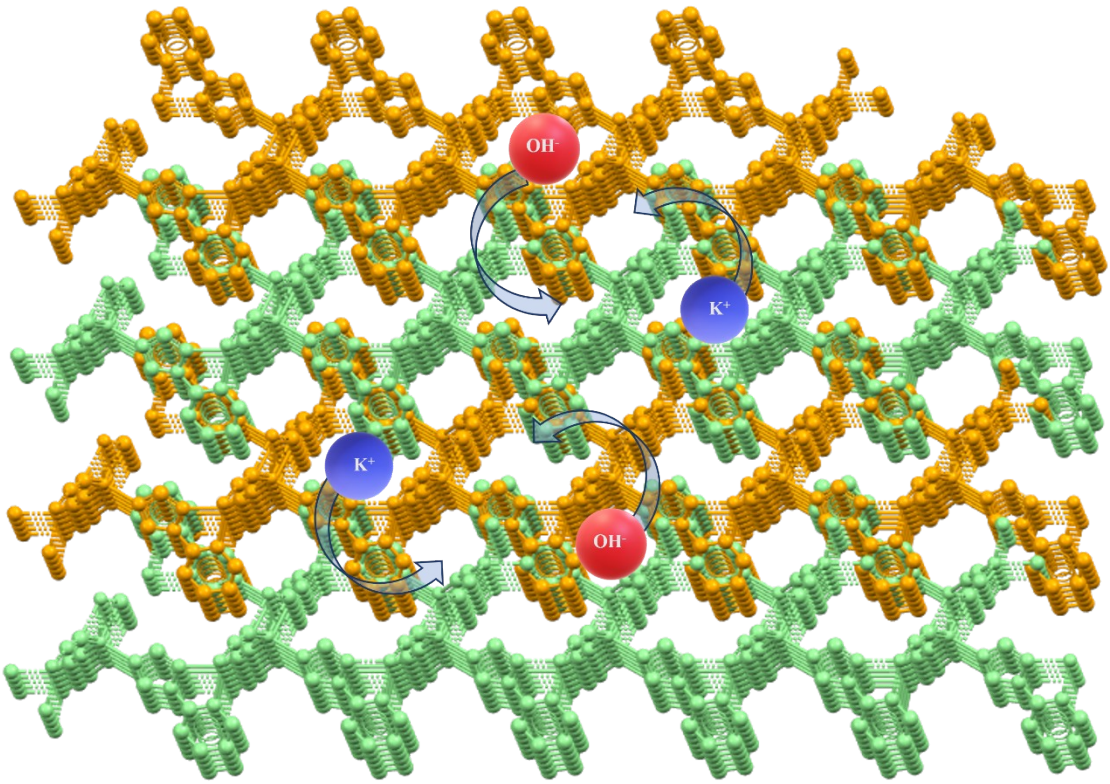

Figure S8. Interlocked layer of MOF (Orange and green colour of different layers) forming a 3D packing

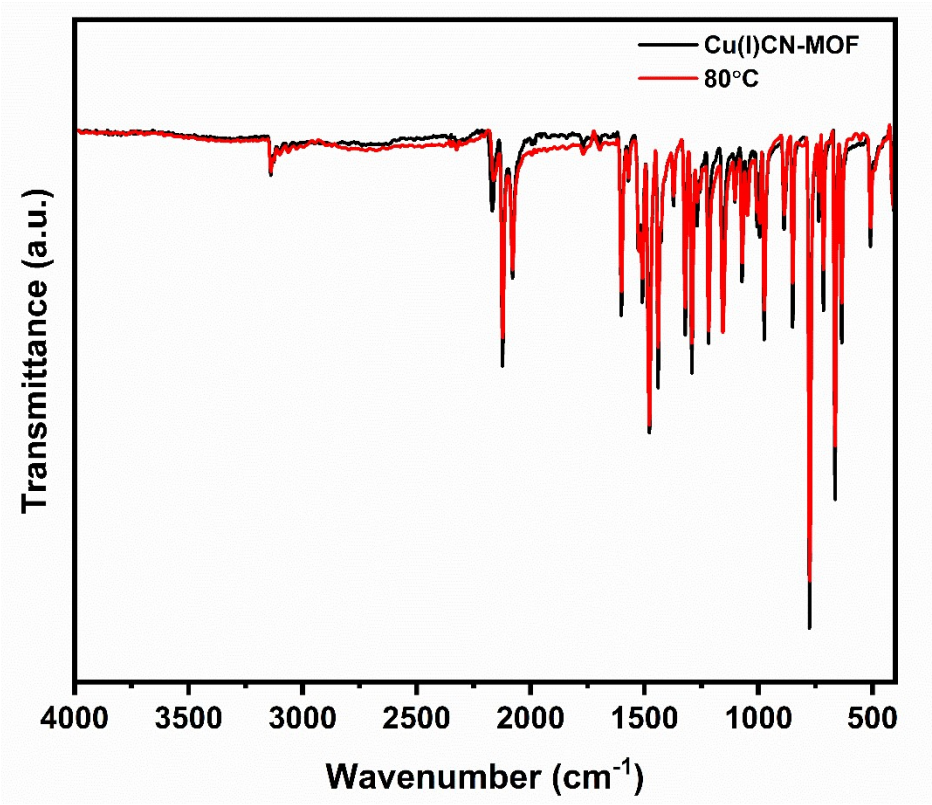

Figure S9. IR data comparison at 25 °C and 80 °C of **CuCN-MOF**.

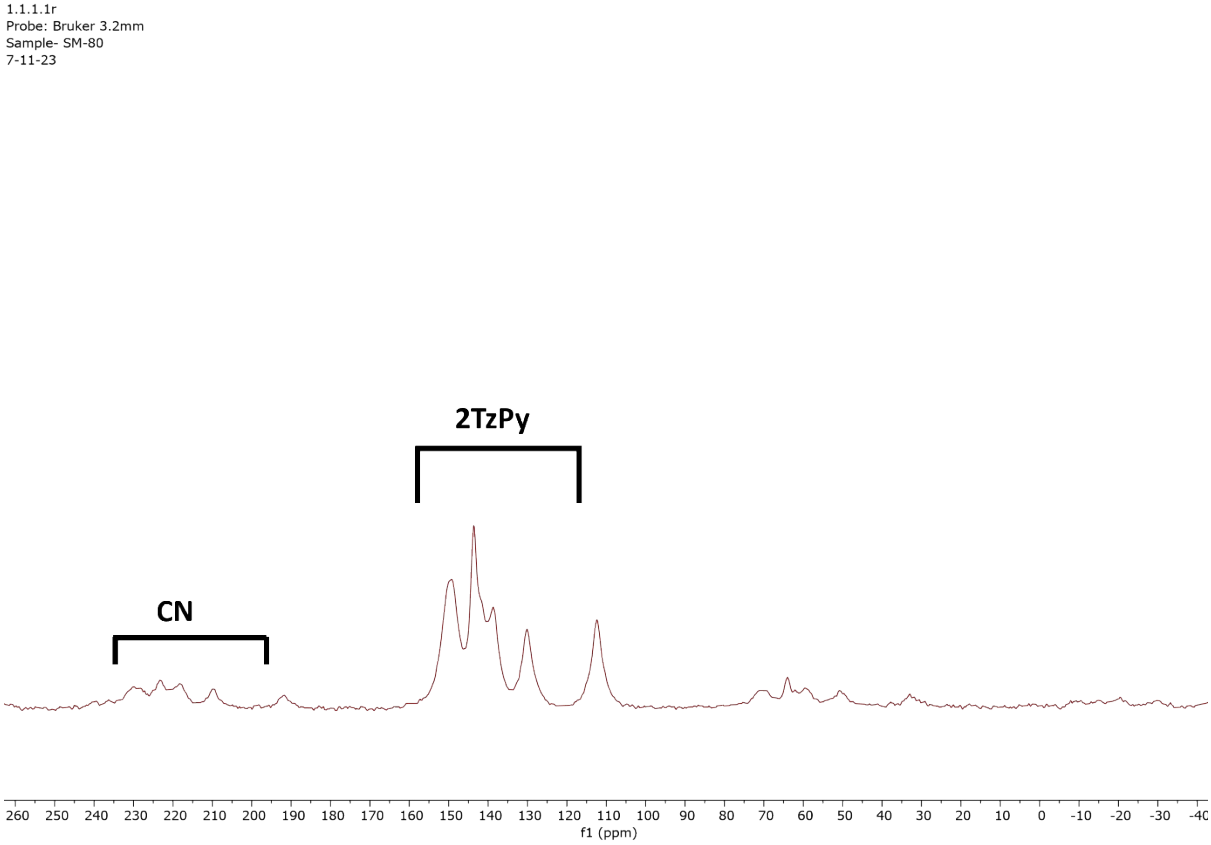

Figure S10. Solid-state ^{13}C CPMAS NMR of **CuCN-MOF**.

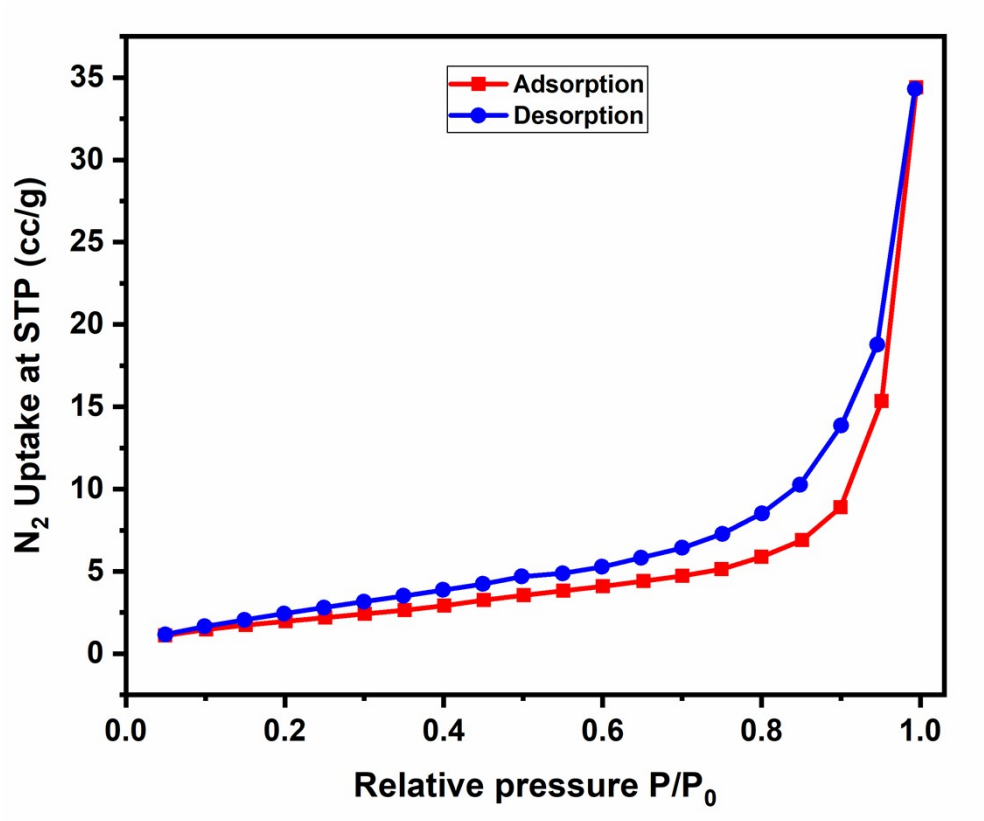

Figure S11. BET isotherm of **CuCN-MOF**.

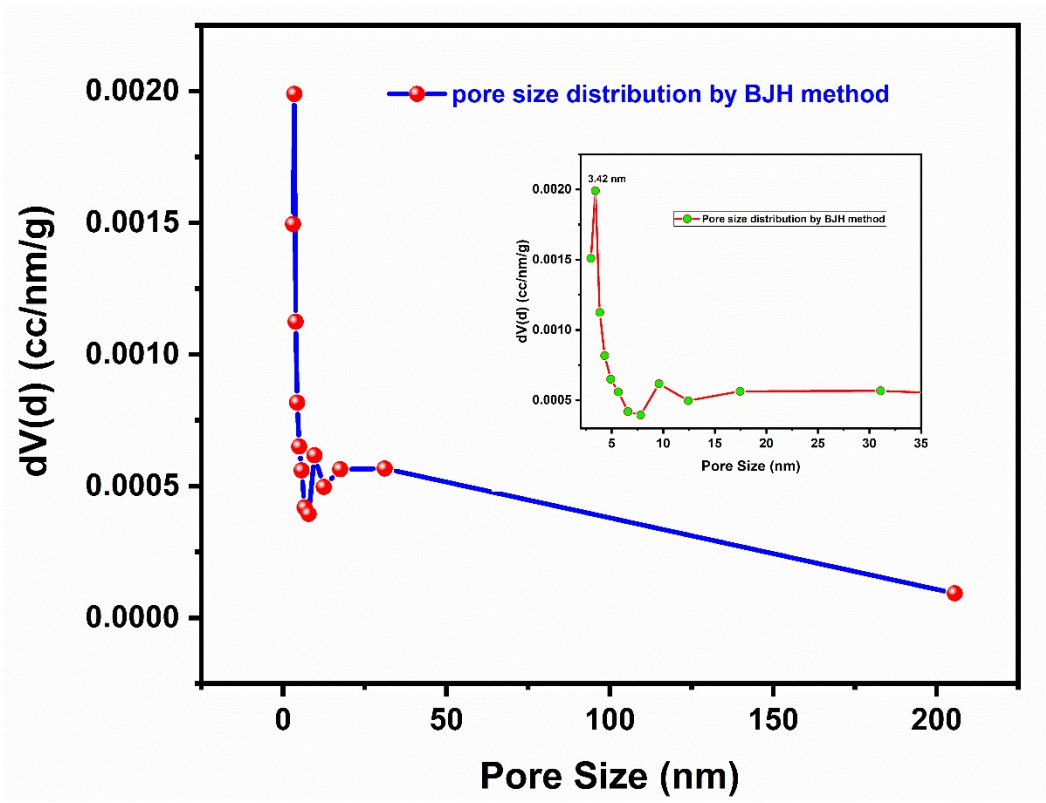

Figure S12. Porosity distribution by BJH method of **CuCN-MOF**.

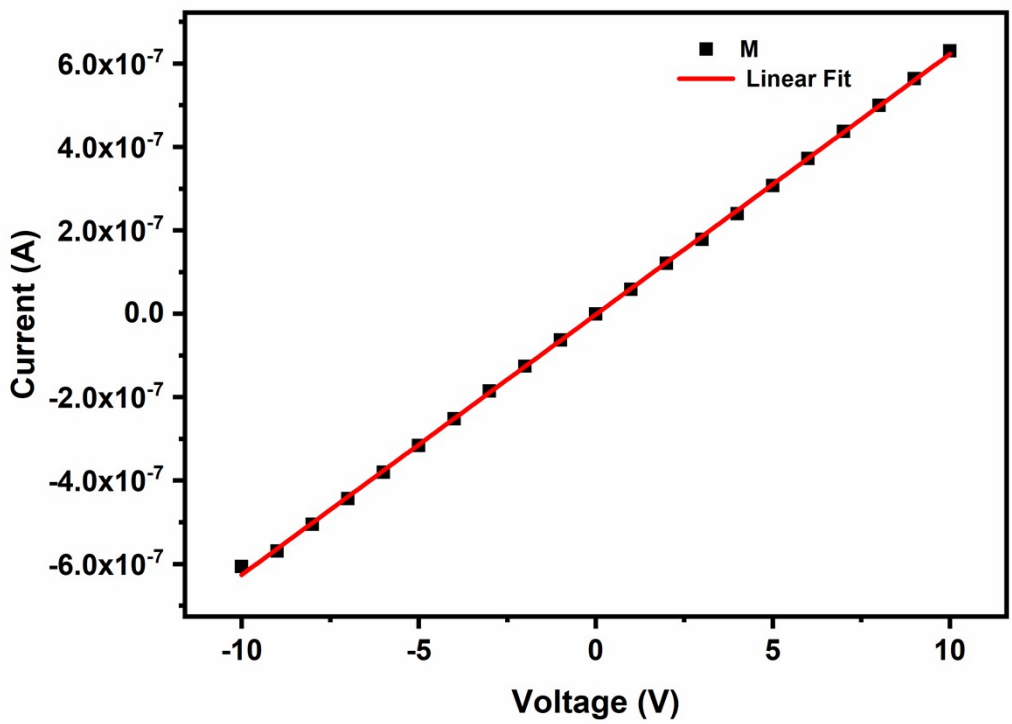

Figure S13. Electrical conductivity of **CuCN-MOF**.

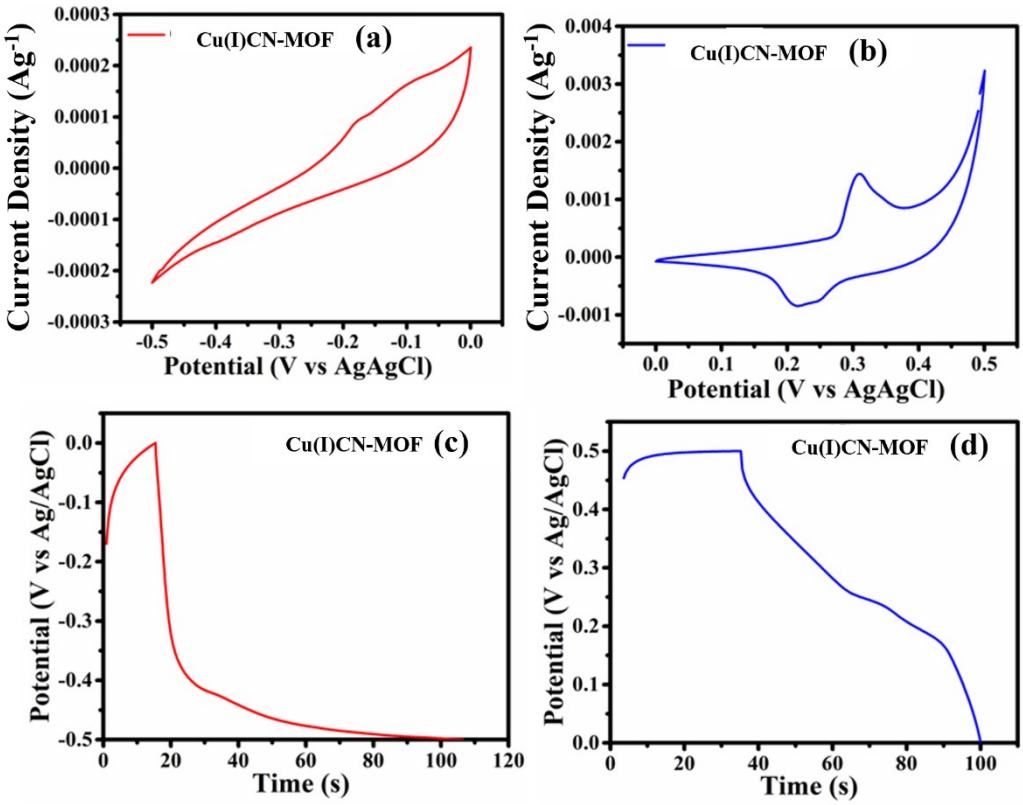

Figure S14. (a-d) CV of **CuCN-MOF** in Negative and Positive range at 10 mVs^{-1} and 1 Ag^{-1} respectively.

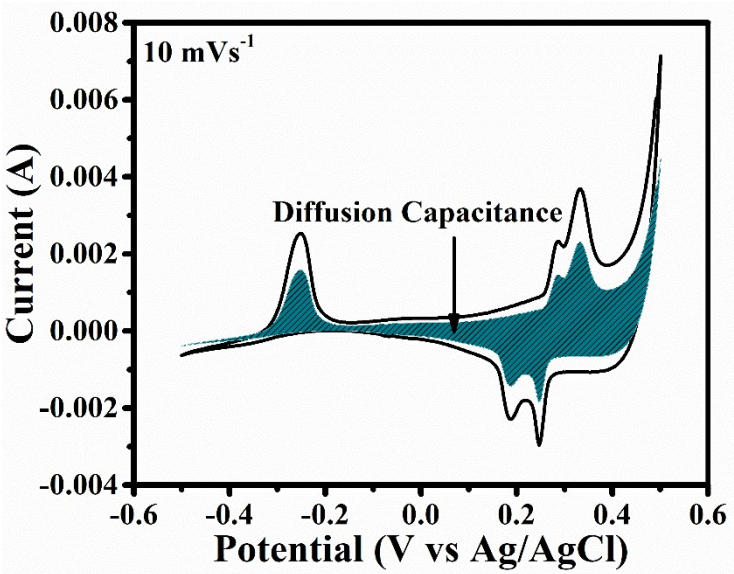

Figure S15. Comparison of calculated CV profile of **CuCN-MOF** for diffusion-only capacity and overall experimental at 10 mVs^{-1}.

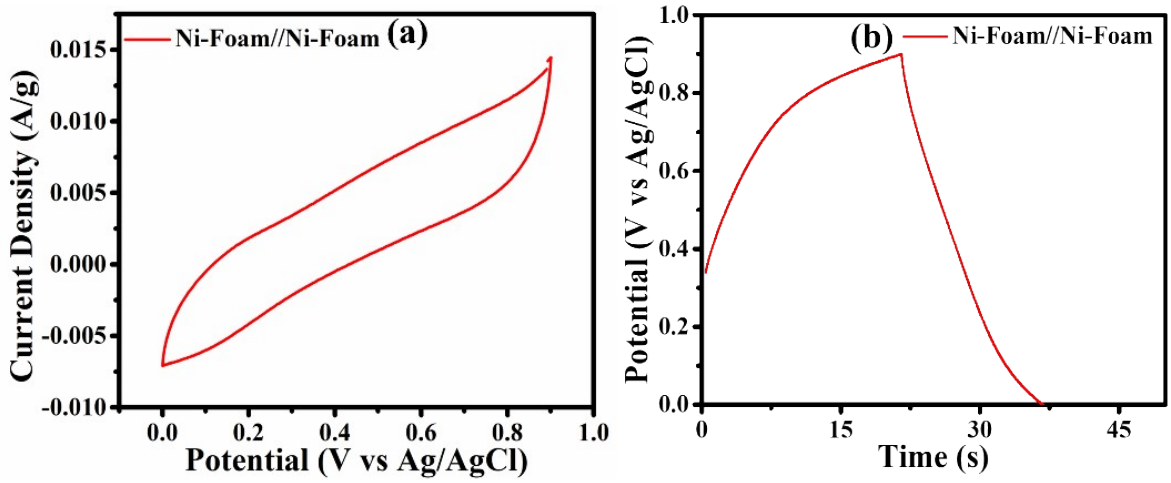

Figure S16. Cyclic voltammogram of Bare Ni-foam.

Table S4. K1 and K2 values for Dunns analysis.

K1- Slope	K2- Intercept
0.46136	-20.25703
0.46813	-16.79191
0.45497	-13.46578
0.4318	-10.11395
0.45141	-7.1348
0.45702	-6.14246
0.46331	-5.31404
0.46365	-4.51793
0.46529	-3.81378
0.46271	-3.16795
0.45447	-2.65597
0.44143	-2.12152
0.44143	-2.12152
0.42625	-1.5916
0.41029	-1.06665
0.38828	-0.48122
0.3591	0.23919
0.33348	1.09321
0.30644	2.28653
0.29447	4.16389
0.12043	-0.91085
0.05517	-2.56164
0.01303	-3.41041

-0.00978	-4.06926
-0.02428	-4.66774
-0.02279	-5.39844
-0.01013	-6.21644
-0.000752	-7.00467
0.01715	-7.86525
0.03557	-8.74799
0.05637	-9.66366
0.08962	-10.74624
0.11908	-11.84978
0.1534	-13.18328
0.18212	-14.63512
0.20302	-16.15424
0.22449	-17.93095
0.30447	-21.26939
0.37359	-24.13267
0.45509	-19.84347

Table S5. Comparison table for efficiency in devices.

Metal complex	**Electrolyte**	**Binder**	**Energy density(Wh Kg^{-1})**	**Specific capacity/capacitance**	**Cycling stability**	**Reference**
Co-MOF	1M KOH	PVDF	23.2	104.3 C g^{-1} @ 1 A g^{-1}	146%, 3000 cycles	4
Ni-MOF	3 KOH/0.1 M, $K_4Fe(CN)_6$	PVDF	55.8	96.7 mA h g^{-1} @ 1 A g^{-1}	90.6%, 3000 cycles	5
Ni-MOF	3M KOH	PVA	4.18 mW h cm^{-3}	230 mF cm^{-2} @1.0 mA m^{-2}	92.8%, 5000 cycles	6
Ni-P-H-MOF	1M KOH	PVDF	63.4	268 C g^{-1} @ 1.6 A g^{-1}	83%, 3000 cycles	7
Fe-**MOF**	6.0M KOH	PTFE	40	121 F g^{-1} @ 1 A g^{-1}	93.1%, 5000 cycles	8
Co(MOSCP)	1M KOH	Free	31.97	102.3 F g^{-1} @ 1 A g^{-1}	73.4%, 5000 cycles	9
Co-Mn-MOF	2M KOH	Free	30.58	106.7 F g^{-1} @ 0.8 A g^{-1}	82%, 3000 cycles	10
Cu-MOF	1M Na_2SO_4	PVDF	30.56	152.79 F g^{-1} @ 0.5 A g^{-1}	90.07 %, 10000 cycles	11
$CuAg_4$(BHT)	1M KCl	Free	17.1	38 F g^{-1} @ 0.5 A g^{-1}	90%, 5000 cycles	12
NAU-1	4.0M KOH	PTFE	100.1	-	>100%, 1500 cycles	13
Cu(I)CN-MOF	6M KOH	Free	62.9	266.5 C g^{-1} @ 1 A g^{-1}	81.1%, 5000 cycles	14
Cu(I)CN-MOF	**1M KOH**	**Free**	**68.175**	**136.48 C g^{-1} @ 1 A g^{-1}**	**96.5%, 10000 cycles**	**This work**

References.

1 O. V. Dolomanov, L. J. Bourhis, R. J. Gildea, J. a. K. Howard and H. Puschmann, *J. Appl. Cryst.*, 2009, **42**, 339–341.

2 G. M. Sheldrick, *Acta Crystallogr A Found Adv.*, 2015, **71**, 3–8.

3 N. Kommu, V. D. Ghule, A. S. Kumar and A. K. Sahoo, *Chemistry – An Asian Journal*, 2014, **9**, 166–178.

4 M. Z. Iqbal, M. M. Faisal, S. R. Ali, S. Farid and A. M. Afzal, *Electrochimica Acta*, 2020, **346**, 136039.

5 Y. Jiao, J. Pei, C. Yan, D. Chen, Y. Hu and G. Chen, *J. Mater. Chem. A*, 2016, **4**, 13344–13351.

6 Y. Yan, P. Gu, S. Zheng, M. Zheng, H. Pang and H. Xue, *Journal of Materials Chemistry A*, 2016, **4**, 19078–19085.

7 M. Z. Iqbal, M. W. Khan, S. Aftab, S. M. Wabaidur and S. Siddique, *Dalton Trans.*, 2023, **52**, 6166–6174.

8 K. Wang, S. Wang, J. Liu, Y. Guo, F. Mao, H. Wu and Q. Zhang, *ACS Appl. Mater. Interfaces*, 2021, **13**, 15315–15323.

9 Y. Ling, H. Chen, J. Zhou, K. Tao, S. Zhao, X. Yu and L. Han, *Inorg. Chem.*, 2020, **59**, 7360–7369.

10 S. H. Kazemi, B. Hosseinzadeh, H. Kazemi, M. A. Kiani and S. Hajati, *ACS Appl. Mater. Interfaces*, 2018, **10**, 23063–23073.

11 S. Krishnan, A. K. Gupta, M. K. Singh, N. Guha and D. K. Rai, *Chemical Engineering Journal*, 2022, **435**, 135042.

12 Y. Jin, S. Wu, Y. Sun, Z. Chang, Z. Li, Y. Sun and W. Xu, *Mater. Horiz.*, DOI:10.1039/D3MH00424D.

13 K. Wang, Z. Wang, S. Wang, Y. Chu, R. Xi, X. Zhang and H. Wu, *Chemical Engineering Journal*, 2019, **367**, 239–248.

14 Y. Jin, S. Wu, Y. Sun, Z. Chang, Z. Li, Y. Sun and W. Xu, *Mater. Horiz.*, DOI:10.1039/D3MH00424D.